Thermal and Vapor Smoothing of Thermoplastic for Reduced Surface Roughness of Additive Manufactured RF Electronics

Clayton NefiG, Eduardo A. Rojas-Nas trucci, *Member, IEEE,* Justin Nussba um, Darrell Griffin, Thomas M. Welleer , *Fellow, IEEE ,* and Nathan B. Crane

Abstract- Additive manufacturing **(AM)** of electronics **provides a route for creating customized systems with novel geometries that are not feasible with traditional methods. Standard AM processes such as extrusion can produce substrates on which electrical traces can be deposited. However, the surface roughness of plastic extrusion reduces the effective electrical conductivity and can introduce anisotropy, especially in radio frequency (RF) devices. The roughness can be reduced using vapor smoothing (VS), but solvent absorption changes the surface composition slightly, can be environmentally hazardous, and is not feasible with all thermoplastics. A new method introduced here-c oined thermal smoothing (TS)- utilizes a heat source to locally reflow the material, thus minimiz ing the roughness of the undulating surfaces without the drawbacks of VS. This research work compares the surface roughness impacts of both smoothing processes with profilometry and scanning electron microscope (SEM) images. Both smoothing processessignificantly reduce the surface roughness of extruded components by 80% and 90% for TS and VS, respectively. This paper also examines the influence of surfacesmoothing on high-frequency conductivity of microdispensed conductors (CB028 paste) deposited on the substrates. The measured loss on coplanar waveguides shows an improvement of up to 40% at 7 GHz.**

Manuscript received February 14, 2018; revised February 14, 2019; accepted March 11, 2019. Date of publication April 11, 2019; date of current version June 6, 2019. Recommended for publication by Associate Editor A. Jain upon evaluation of reviewers' comments. *(Correspo11di11g author: Clayton Neff.)*

C. Neff was with the Department of Mechanical Engineering, University of South Florida, Tampa, FL 33612 USA. He is now with the National Research Council, Air Force Research Laboratory, Eglin Air Force Base, Valparaiso, FL 32542 USA (e-mail: claytonneff@mail.usf.edu).

E. A. Rojas-Nastrucci was with the Electrical Engineering Department, University of South Florida, Tampa, FL 33612 USA. He is now with the Electrical, Computer, Software and Systems Engineering Departmen,tEmbry-Riddle Aeronautical University, Daytona Beach, FL 32114USA.

J. Nussbaum was with the Department of Mechanical Engineering, University of South Florida, Tampa, FL 33612 USA. He is now with the Oak Ridge National Laboratory, Oak Ridge, TN 37830 USA.

D. Griffin was with the Department of Mechanical Engineering, University of South Florida, Tampa, FL 33612 USA. He is now with Pall Corporation, New Port Richey, FL 34654 USA.

T. M. Weller was with the Electrical Engineering Department, University of South Florida, Tampa, FL 33612 USA. He is now with the School of Electrical Engineering and Computer Science, Oregon State University, Corvallis, OR 97331 USA.

N. B. Crane was with the Department of Mechanical Engineering, University of South Florida, Tampa, FL 33620 USA. He is now with the Mechanical Engineering Department, Brigham Young Universtiy, Provo, UT 84602 USA.

Color versions of one or more of the figures in this paper are available online at http://ieeexplore.ieee.org.

Digital Object Identifier 10.1109/TCPMT.2019.2910791

***Illdex* Terms- Additive manufacturing (AM), conductive ink, coplanar waveguide (CPW), printed electronics, surface roughness, thermal smoothing (TS), vapor smoothing (VS).**

I. INTRODUCTION

ADDITIVE manufacturing (AM) refers to a set of processes that enable fabrication of components directly from digital models using controlled material deposition or fusing [l], [2]. **AM** processes have advantages including increased geometric freedom, reduced cost of customization due to eliminating part-specific tooling, and reduction in waste material [l], [3]- [5].New hybrid AM methods merge conductive ink microdispensing, computer numerical control machining, laser machining, and pick-and-place technologies in order to fabricate functional electronics [6]- [8]. However, many AM processes have significant limitations including anisotropy, lower than bulk material properties, and higher surface roughness [9]- [16].

While photolithography provides fine resolution, excellent electrical performance, and high integration density, it also requires expensive equipment, part-specific tooling (masks), and is largely limited to flat substrates [17], [18]. Pbotolithography also can entail many deposition and etching steps generating a considerable amount of waste, infrastructure needs (e.g., a cleanroom), labor, and processing time. Hybrid AM methods have the potential to overcome these limitations and are particularly attractive in radio frequency systems and low-cost electronics (antennas, waveguides, RFID tags, smart cards, and sensors), where characteristic geometries are > 10 μm, electrical requirements are not as demanding, and there are potential performance benefits from a 3-D geometry [18]-[27].

The application space for hybrid printed electronics is constrained by the electrical performance of the systems (e.g., the dissipative loss). The main limitation is the effective electrical conductivity of the 3-D-printed inks. Many of the commercial inks have de conductivity two orders of magnitude lower than pure silver [28], [29]. Moreover, the roughness of the printed substrates further degrades the electrical properties by increasing dissipative losses-e specially at higher microwave frequencies [30]- [33].

The surface roughness of plastic extrusion within the realm of **AM** ranges anywhere from ~2 to 50 μm depend-

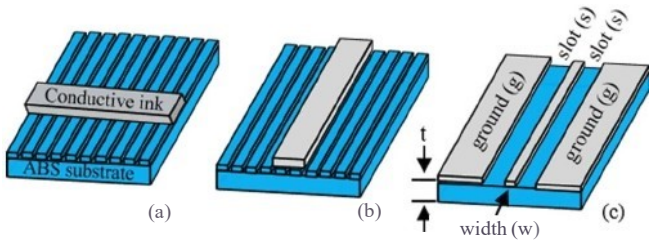

Fig. 1. Directionality of undulating extruded surfaces with (a) perpendicular and (b) parallel dispensed conductive ink and (c) diagram of CPW.

ing on print orientation and settings [9], [12], [34], [35]. Hawatmeh *et al.* [36], Stratton [37] show the insertion loss of microstrip lines can vary by more than 30% when considering the orientation of plastic extrusion for the undulating surfaces seen in AM, illustrated in Fig. 1 as perpendicular and parallel. It is evident that the undulating surfaces can directly hinder the performance of functional electronics by increasing conductor effective length thus insertion loss, and may also introduce open circuits from over-extrusion or short circuits from under-extrusion when conductive ink is microdispensed on top of the undulating surfaces [7], [28].

This paper considers the impact of postprocessing methods to reduce surface roughness. Vapor smoothing (VS) has been shown to significantly reduce surface roughness of extruded components while maintaining dimensional accuracy [34], [35], [38]-[41]. In VS, the part is exposed to a solvent vapor. The solvent in the atmosphere is absorbed, and the material locally reflows due to surface tension and gravitational effects- yielding a much smoother surface finish. The most common method utilizes acetone vapor to treat acrylonitrile butadiene styrene (ABS). While VS is a low-labor, proven process, it is not feasible with all thermoplastics, it leaves residual solvent that may alter material properties [35], and the solvents have an environmental impact.

VS will be compared with a new postprocessing method called thermal smoothing (TS). This method utilizes an optical source to beat the surface. TS is applicable to all thermoplastics, does not alter material composition, enables spatial control of smoothing and quick processing, and eliminates the environmental issues with solvent use. Perhaps most importantly, it can be integrated into an AM system for treating intermediate layers as well as the final exposed surfaces-which could be useful where electronics are to be embedded within a structure. This paper reports the impacts of VS and TS with a reduction up to 90% of the undulating surface roughness of extruded components. A study of microdispensed coplanar waveguides (CPWs) [Fig. l(c)] shows the potential benefits of smoothing processes by measuring the electrical performance with and without smoothing treatments and with varied orientation of the conductor relative to the extrusion paths. Smoothing processes improve the electrical performance by reducing dissipative losses up to 40% depending on CPW orientation.

II. METHODS

Substrates 25 x 25 mm^2 were fabricated using 3DXTech Jet Black ABS in two different machines. An open-source printer with a 400-μm-diameter nozzle fabricated the "RepRap" substrates to a thickness of 2 mm using 200-μm-layer heights. A nScrypt Table Top 3Dn system fabricated the "nScrypt" samples as an example of higher quality substrates using a 250-μm-diameter nozzle and a final thickness of 1 mm using 100 - μm-layers. The nScrypt components were only 1 mm in thickness since they could easily be removed from the bed without warping and decreased the print time by about 50%. Both substrate types were printed with 0° raster angle, 100% infill, 230 °C extrusion temperature, and 100 °C bed temperature to match printing conditions on both machines. Six substrates were fabricated for each subset of testing including untreated, VS, and TS for both RepRap and nScrypt substrates, for a total of 36 substrates. For *RepRap* samples only, CPWs were deposited on the surface with three samples oriented perpendicular and three parallel to the extrusion paths. Once substrates were printed, the surface topology was characterized using a Veeco Dektak 150 profilometer. A 5-μm-radius tip was used on the contact stylus with 3 mg of contact force and a spatial resolution of 8 and 0.278 nm in the vertical roughness and horizontal scan directions, respectively. Each substrate was scanned along three different lines, each perpendicular to the polymer extrusion paths with a scan length of 5 mm in 60 s. The average *(Ra)* and rms *(Rq)* surface roughness were recorded for each scan and averaged for an overall average and rms roughness. A cutoff length of 1 mm was utilized to attenuate low-frequency "waviness" of the substrates. After smoothing processes were performed, surface roughness was measured and compared to the untreated substrates before performing the electrical characterization. The fabrication process flowchart is shown in Fig. 2.

A. Substrate Postprocessing

VS was performed by placing two substrates at a time on a sample bed within a 472-mL container in ambient laboratory conditions. With the substrates in position, 5 mL of liquid acetone was introduced to the bottom of the container that was then sealed for 50 min as illustrated in Fig. 3(a). After the 50-min cycle, substrates were removed and allowed to dry in ambient laboratory conditions for at least 24 h before further processing.

TS subjects the substrate to localized beat. In this work, the localized beat radiated from a modified projector emitting high-intensity visible light to heat the surface. This system has also been used to fuse entire layers of polymer powder as an alternative to laser sintering; more details can be found in [42]. The beat patterning device from this process enables surface smoothing in this work by patterning heat over a 21 x 16 mm^2 (4:3 aspect ratio) exposure area on the top surface. This elevates the temperature only in the exposure area, allowing the material to reflow and self-smooth by surface forces. A FLIR infrared **(IR)** camera (model #: A325sc) captured temperature versus time data during the smoothing process. The TS experimental setup is illustrated in Fig. 3(b). The substrate was subjected to a low-intensity preheat of 0.76 W/cm^2 for 60 s where the top surface reached 150 °C, which may be an approximate temperature

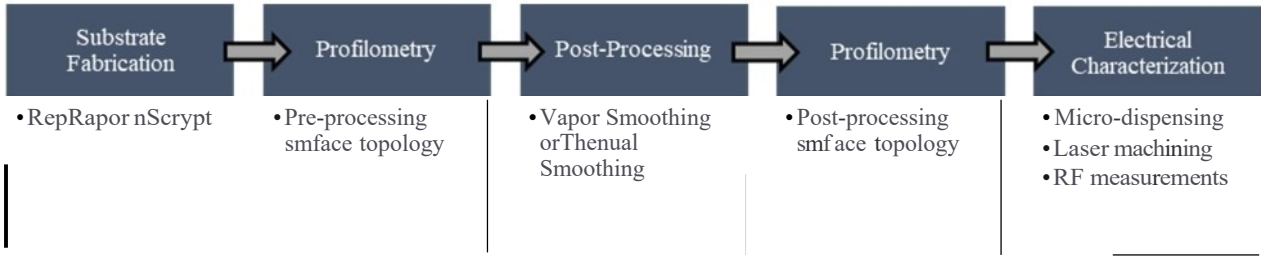

Fig. 2. Process flowchart for substrate fabrication, surface topology measurements, postprocessing, and electrical characterization.

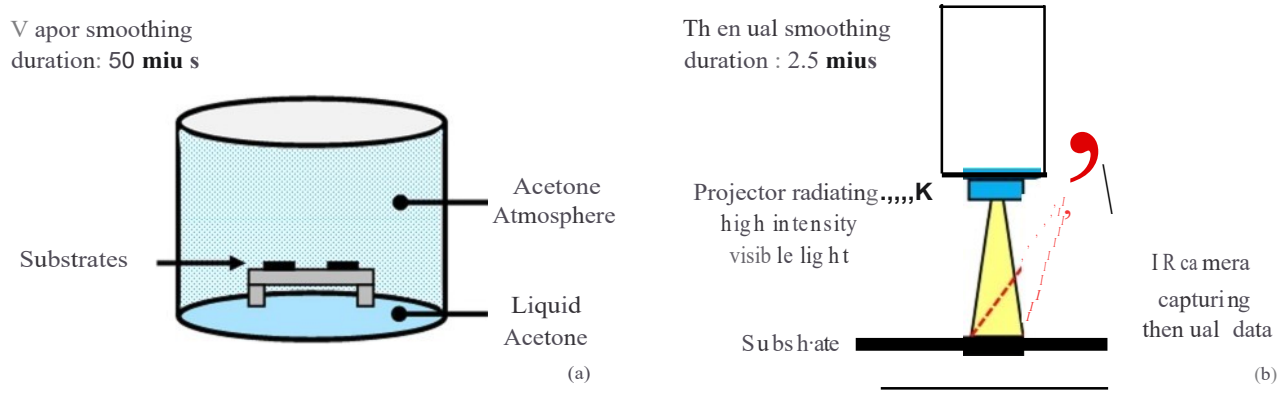

Fig. 3. Postprocessing methods. (a) VS. (b) TS.

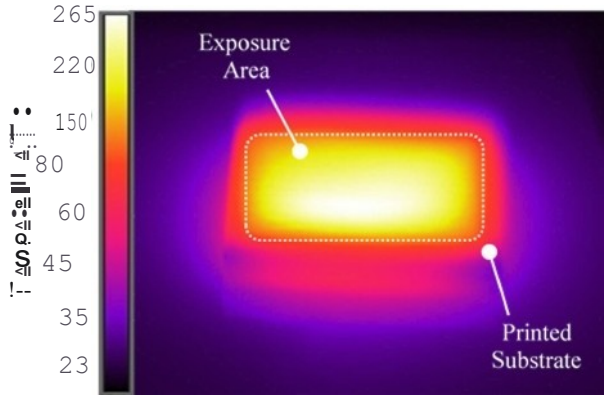

F ig. 4. Thermal image from IR camera during TS.

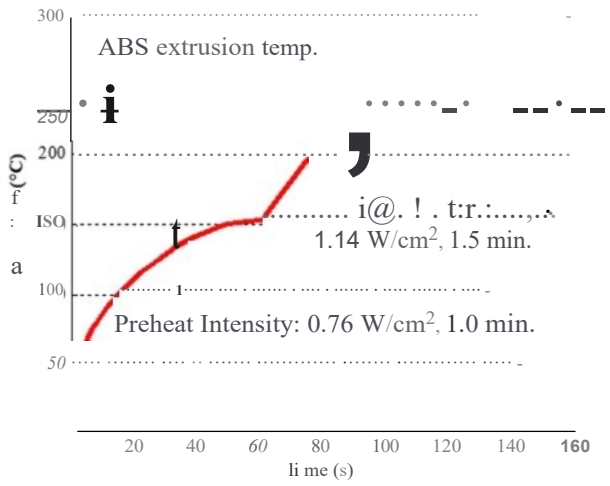

Fig. 5. TS temperature versus time profile.

of the printed surface just after extrusion in an *in situ* TS operation. The power was then increased sharply to near full intensity of 1.14 W/cm^2 for 90 s to raise the surface temperature over the ABS extrusion temperature to smooth the surface. Preheating also reduces thermal gradients and eliminated warping during treatment. A thermal image in Fig. 4 shows the spatial distribution of temperature just before the TS process ended. Fig. *5* illustrates the complete temperature versus time profile of the TS process.

B. Electrical Characterization

A CPW transmission line with 50-Q characteristic impedance was designed and laser-machined from a conductor with overall conductor dimensions of 7.5 x 3.68 mm^2 [Fig. l(c)]. The nScrypt SmartPump was used to microdispense CB028, a commercially available silver thick-film paste from DuPont, as the conductor on the *RepRap substrates only*. The parameters of the CB028 rnicrodispensing are 175 µ m/125 *µm* ceramic tip, printing speed 25 mm/s, printing pressure 12 psi, dispense gap of 100 *µm* between the ceramic tip and substrate, and valve opening 0.1 mm. The dispense gap was set by contacting the substrate with the ceramic tip and then offsetting the tip vertically by 100 *µm*. For the untreated substrates with large undulations, the contact point was on a peak of the undulated surface. Furthermore, the CPWs

TABLE I

SURFACE ROUGHNESSOF R EPR AP AND NSCRYPT SAMPLES

Surface Roughness (µm)	RepRap			nScrypt		
	Untreated	Thermal Smoothing	Vapor Smoothing	Untreated	Thermal Smoothing	Vapor Smoothing
R..	10.53 ± 1.22	2.00 ± 0.15	0.79 ± 0.11	3.88 ± 0.35	0.92 ± 0.08	0.60 ± 0.08
R.	12.73 ± 1.46	2.42± 0.21	0.98 ± 0.16	4.81 ± 0.34	1.16 ± 0.12	0.72 ± 0.09

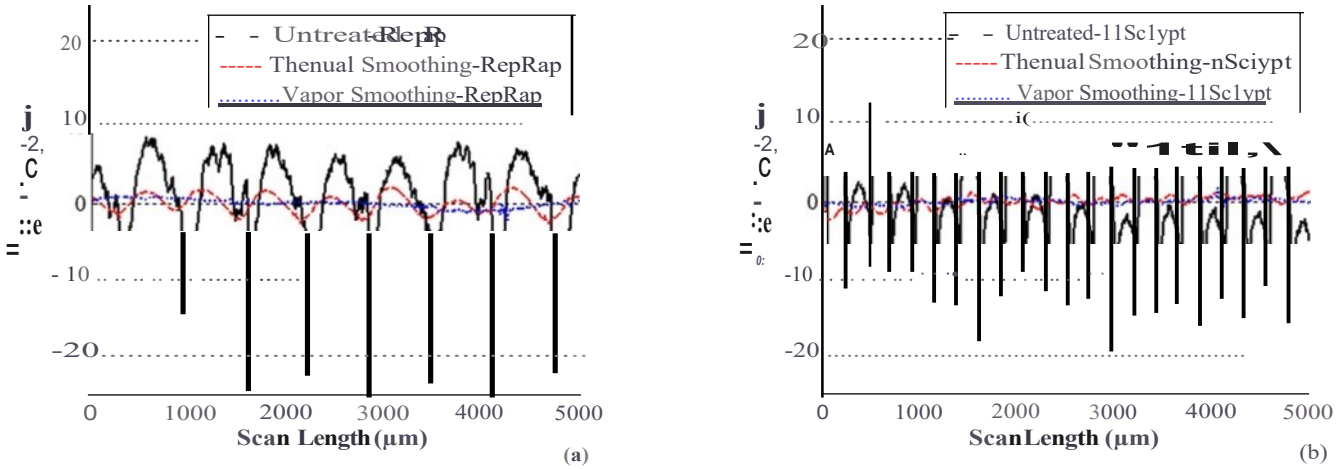

Fig. 6. Profilometry data of untreated, TS, and VS surfaces for (a) *RepRap* and (b) *nScrypl* samples.

were dispensed perpendicular and parallel with respect to the extrusion paths for performance comparison. After dispensing, the samples were cured in a box oven at 80°C for 60 min. A Lumera Super Rapid picosecond laser, operating at 1064-nm wavelength with < 15-ps pulsewidth, is then utilized to cut two slots into the conductor, thereby forming two ground planes and a signal line in the center. (The laser settings are 1-W average power, seven repeated passes, and a repetition rate of 100 KHz.) The final measured dimensions are 379.50± 11.69 μm, 66.87± 5.12 μm, and 1.67± 0.07 mm for the center linewidth (w), slot size (s), and ground width (g), respectively, as denoted in Fig. l(c). The thickness (t) of the substrate (ABS) is 2 mm as denoted in Fig. l(c). The performance characterization is based on S-parameters that are measured with a vector network analyzer Agilent N5227A **PNA.** For this, a pair of 1200-µ m-pitch ground-s ignal-ground (GGB Industries ECP18-GSG-1200-DP) probes are utilized. Calibration is performed using a GGB CS-10 calibration substrate.

III. RESULTS

A. Surface Smoothing

Table I indicates that both smoothing processes diminish the magnitude of the undulating surfaces and that the vapor polishing produced a lower final roughness than the TS. Untreated nScrypt components have tighter trenches between extrusions, resulting in a lower initial roughness than the untreated RepRap components. Thus, the smoothing effect is more pronounced for the RepRap components as more material will reflow during smoothing. TS reduces *Ra* of RepRap components to 2 μm, while TS nScrypt components and VS (regardless of component type) achieves an *Ra* of under 1 μm.

Profilome try scans shown in Fig. 6 and scanning electron microscope (SEM) images shown in Fig. 7 show the comparable surface topology of the RepRap and nScrypt components. A feature to emphasize is the wider trenches between untreated RepRap extrusions, whereas untreated nScrypt components have a much tighter trench. This could partly explain the difference in *Ra* even though the peaks of the untreated nScrypt extrusions are close to the same height of the untreated RepRap extrusions. It is possible that the full depth of the trenches and resulting *Ra* is not fully measured due to the limitation of probe size, which would have a greater effect on the nScrypt samples since the trenches are narrower. Either a smaller profilometer probe size, optical measuring equipment, or atomic force microscopy may be able to yield more accurate surface feature measurements but the overall trends would likely remain the same. Figs. 6 and 7 also illustrate TS reduces the height of the undulating roughness corresponding to extrusion lines but does not eradicate the wavy features as fully as VS. Untreated nScrypt components have sharper radii for extrusions from the characteristically smaller nozzle diameter, but Figs. 6(b) and 7(d) show that there is a process error as the surface peaks have alternating heights of about 4 and 12 μm. Smoothing processes erase the process error artifact.

B. Electrical Performance

Fig. 8 shows the experimental results for average attenuation constant (a) and phase constant (/J) versus frequency for each

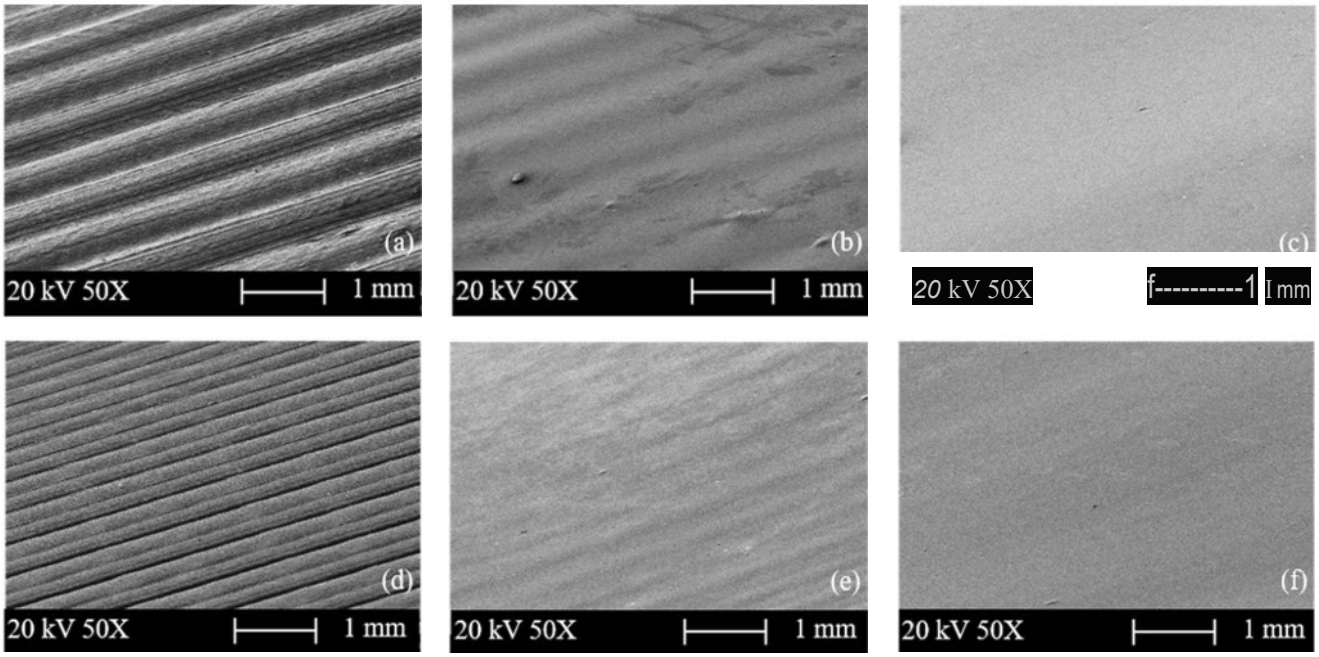

Fig. 7. SEM images at SOX of (a) untreated RepRap, (b) TS RepRap, (c) VS RepRap, (d) untreated nScrypt, (e) TS nScrypt, and (f) VS nScrypt.

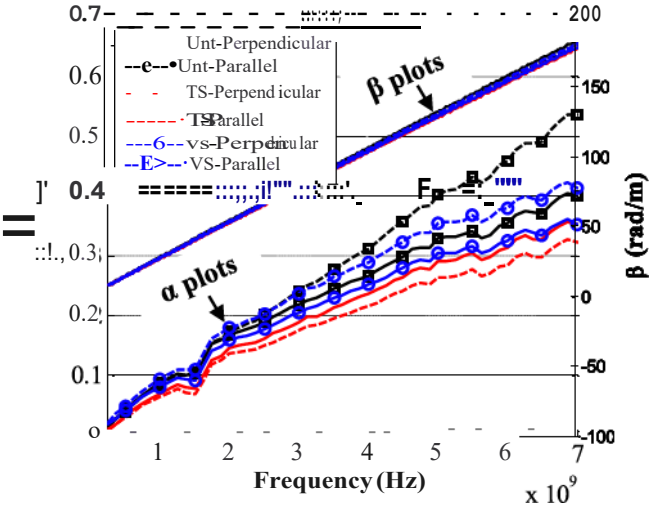

Fig. 8. Experimental results of average attenuation constant (a) and phase constant (P) versus frequency of parallel and perpendicular CPWs printed on RepRap substrates. Note: Unt = untreated, TS = thermal smoothing, VS = vapor smoothing, and perpendicular and parallel denote the CPW orientation in relation to the undulated extrusion paths.

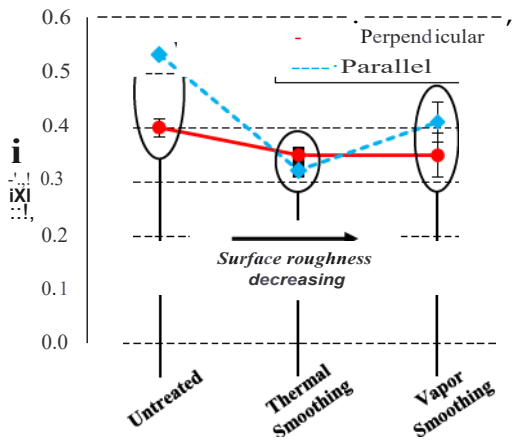

Fig. 9. Average attenuation constant *(a)* at 7 GHz with standard deviation for both conductor orientations for the RepRap substrates. Note *a* becomes nearly isotropic upon TS while VS has significant variation. Also, untreated extruded substrates have the largest loss and discrepancy between conductor orientation.

substrate subset, while Fig. 9 shows the average a and $/J$ with standard deviations at 7 GHz. We analyze the propagation constant $y = a + j/J$, as it provides a metric to quantify the effect that surface roughness has on the performance of the transmission lines at microwave frequencies [8], which is computed using the measured S-parameters. The attenuation constant accounts for the dissipative losses per unit length (dB/cm) of the waveguide, whereas the phase constant is related to the wave velocity (rad/m). Experimental results indicate that untreated surfaces have high attenuation constants as the frequency approaches 7 GHz, thus the largest resistance to the transmission of the high-frequency signals for both the perpendicular and parallel CPWs.

The skin effect, which describes the tendency for electrical current to concentrate closer to the "skin" of the conductor as the frequency increases [32], is the driving phenomenon of the current flow characteristics. The skin effect promotes high-current-density regions where cross-sectional area is a minimum as surfaces with electrical current are in close proximity. For current flowing perpendicular to undulating surfaces, the current travels a wavy path that conforms to the features mostly between the peaks of the undulating substrate and the conductor surface due to the skin effect. Hence, current will have high density over the peaks of the undulating

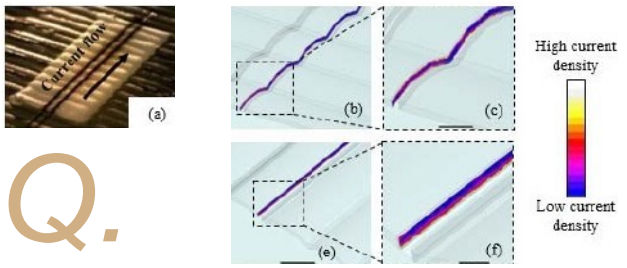

Fig. 10. Current density characteristics along the edge (side view) of the center signal line for (aH c) perpendicular and (dHf) parallel CPWs. Note that the high-current-density areas accumulate over the undulated peaks for perpendicular CPWs, while the high current density is along the bottom edge of the CPW where the cross-sectional area is minimum due to a sharp comer.

surface, as shown in the illustrationsof Fig. lO(b) and (c). This increases effective conductor length and resulting dissipative losses , but not as substantially as in the case of the current conforming to full undulating features, accumulating in the valleys, and having a much more pronounced semicircular current path. Conversely,current flowing parallel to undulating surfaces accumulates along the bottom edge of the centerline conductor, as shown in Fig. lO(e) and (f). Current collects here as the sharp comer along the bottom edge of the center signal line is where the area is at a minimum for the constant cross section, as shown in the cross section of Fig. ll (d). This confines the current to a small region and increases the effective resistance and the resulting dissipative losses of the current path.

Smoothing processes should mitigate the current flowing irregularities due to the undulated features creating a smoother, more ideal current path. Fig. 8 shows both TS and VS significantly decrease dissipative losses. Decreased undulating surface features (as shown in Fig. 11) allow current to flow in a smoother fashion for more ideal flow by conducting through a greater cross-sectional conductor area, which reduces the effective conductor resistance. Fig. 9 depicts the **TS** has nearly isotropic performance between waveguide orientations, which is attractive for designing circuits on extruded surfaces as electrical performance is no longer orientation dependent.

VS also reduces conductor loss comparing untreated components; however, despite the significantly reduced surface features, has much more sample to sample variation than its rougher TS counterparts, as shown in Fig. 9. Furthermore, Fig. ll(c) and (f) proides the evidenceof cracks in the CPWs and substrate. Fig. 12 illustrates the characteristic crack locations on the CPWs. These artifacts are exclusive to the vapor smoothed substrates and so the cracking likely arises from the acetone. It is possible that acetone remaining after the VS process [35] affects microwave signal transmission and impacts the permittivity of the substrate, which makes the electrical performance more unpredictable and less favorable for printed electronic systems.

Other parameters that could affect the conductor loss are the average thickness, thickness variations, and silver ink particle distribution of the conductive layer [8]. Fig. 13 shows that the conductor layer thicknesses range from ~40 to 60 μm for the treated samples when analyzing cross-sectional images of the CPWs. The untreated samples, on the other hand, show a larger variation in thickness (Fig. 13) due to the paste nature of the CB028 and its interaction with the wavy surface. The large variation in conductor thickness could be inducing unpredictable changes in the conductive ink, bow the ink dries, and the morphology, for instance, that could impact the loss and the directional dependence of the CPW orientation with respect to the undulated surface. Although, as discussed, many factors can affect the overall loss of the line, it is observed that untreated samples have higher losses than the treated samples, based on the measured results and simulations of the current distributions on rough substrates. It is also evidenced that VS generates microcracks and more variability in loss in the CPW than when using the thermal smoothed substrates.

IV. DISCUSSION

In this paper, we found that both TS and VS significantly improve surface roughness of extruded ABS for printed electronics or other applications. Both smoothing processes have a similar end surface roughness between RepRap (large nozzle diameter) and nScrypt (small nozzle diameter) components. Smoothing processes impact the larger nozzle diameter components more since larger trenches exist between the extrusion paths, which require greater reflow of the material before creating a uniform surface.

TS bypasses the drawbacks of VS by introducing a process that is compatible with all thermoplastics, does not alter material composition, and offers precise control of smoothing, quick processing, and a green technology with much less environmental impact. TS also could more easily be integrated into an AM system. A concentrated heat source could be in the form of a standalone unit or a tool-head within a multitool **AM** system in which the component being printed can be smoothed in between layers or after print completion for an *in situ* process. This approach may increase fabrication time but would use less energy than a cooled component as the material is already heated from being just extruded by the nozzle.

In a previous work, VS was shown to have a slight impact on mechanical properties including stiffness, strength, and elongation to failure [35]. However, the impacts on the mechanical properties were minimal since VS is a surface-mediated effect and does not enhance the bonding of printed layers throughout the volume of printed component [35]. TS, on the other hand, may provide more beneficial mechanical property impacts by densifying and strengthening the material throughout the volume of a printed component if implemented layer by layer.

During an *in situ* smoothing process, TS has the potential to fuse stacking extrusion layers with enhanced bonding to provide increased mechanical performance while also decreasing the surface roughness. This would increase mechanical properties such as strength, stiffness, and ductility, which are usually inferior to traditionally manufactured components. TS, thus, has the potential to reduce the discrepancy of mechanical properties between AM and traditional manufac turing while also creating more isotropic printed components. A higher power heat source could potentially boost TS to be on par

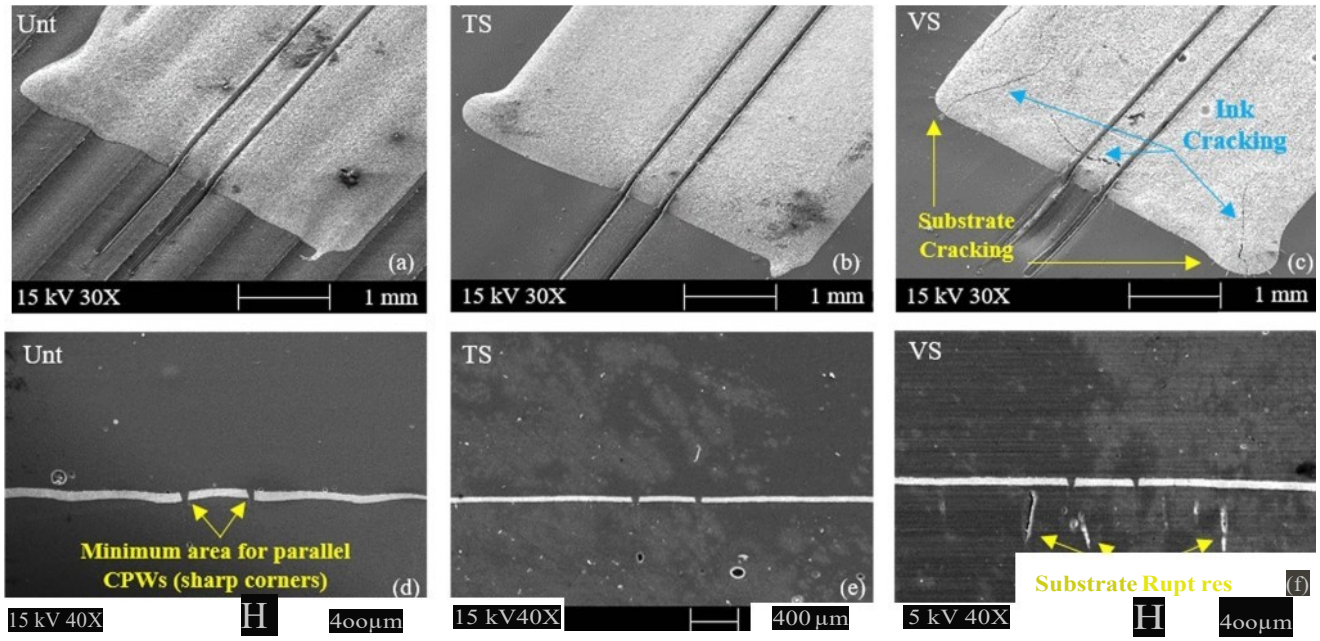

Fig. 11. SEM isometric parallel CPWs: (a) untreated, (b) TS, and (c) VS; and cross sections: (d) untreated, (e) TS, and (t) VS. Note Uni = untreated, TS = thennal smoothing, and VS = vapor smoothing.

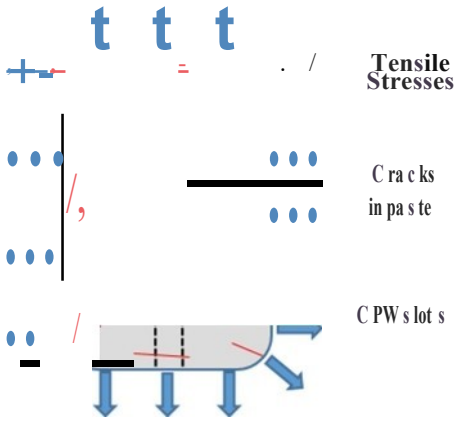

Fig. 12. Illustration of crack locations in vapor-smoothed CPWs. Note that the cracks fonning perpendicular along the edges and radial at the comers where tensile stresses are acting in orthogonal directions.

with VS for surface roughness. In this paper, the intensity was limited to 1.14 W/cm^2, but if a higher intensity heat source was available, the undulating features may diminish more fully in shorter times. However,thin components may be of concern as the large temperature gradients may induce warping. An *in situ* TS process within an **AM** system could be utilized to locally smooth and potentially reduce stresses in the printed parts.

In applications like printed electronics, the inherent surface roughness is a critical obstacle that hinders electrical performance. Undulating surface features can also result in open or short circuits when either over-extruding or under-extruding plastic, respectively. Attempting to eliminate over- or under-extrusion without smoothing processes can lead to time-consuming fine-tuning of the extrusion parameters during fabrication. The idea of structural electronics may benefit from smoothing processes even more as surface roughness on inclined surfaces is more pronounced than top surfaces.

The cracking observed in vapor smoothed components (Fig. 12) could be a significant source of the reduced electrical performance relative to thermal smoothed components. The crack formations are consistent with tensile stresses acting to separate the paste, but the mechanism for the cracking and the role of VS is unclear. Additional work is required to understand this issue, but we posit three potential mechanisms: 1) shrinkage associated with evaporation or residual acetone; 2) environmental stress cracking (ESC) due to acetone presence; and 3) an increased coefficient of thermal expansion (CTE) mismatch between paste and substrate. Acetone evaporation during curing would permit shrinkage of the ABS substrate (especially upon cooling) and increase the stresses in the CPWs. ESC results in a synergistic effect of the chemical agent and mechanical stress that results in crack formation at reduced st ress levels in plastics [43]. In ESC, the chemical agent (in this case acetone) interferes with intermolecular binding, which accelerates molecular disentanglement and eventual fracture at reduced levels [43]. An increase in CTE of the substrate with the addition of acetone could provoke more expansion of the substrate and, in turn, increase the tensile stresses induced in the CPWs. The residual acetone may also be reacting with the solvent in the paste upon curing and inducing the cracks in the paste and ruptures in the substrate. In the future tests, the surface composition of the polymers should be studied to help clarify the source of the cracks and electrical performance degradation.

As the operating frequency of electronic components inevitably continues to rise, smoothing processes can have a substantial impact on permitting printed electronics to infiltrate into widespread application. For instance, Fig. 8 shows the

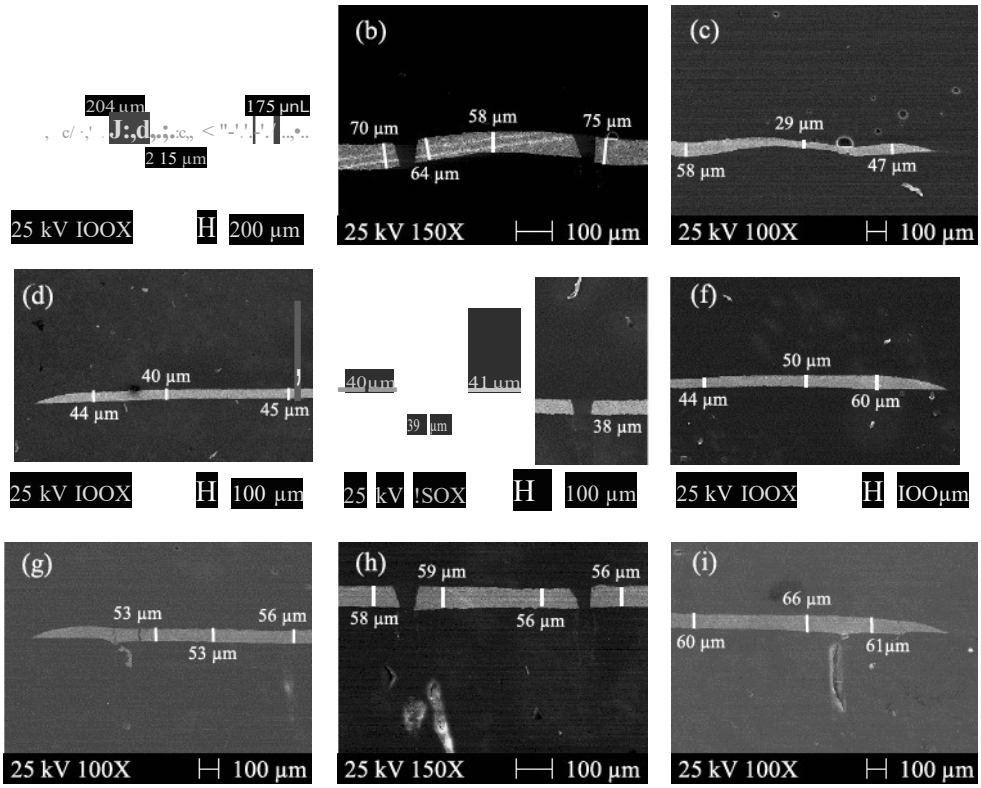

Fig. 13. SEM cross-sectional images of the CPWs. (a) Untreated- left ground. (b) Untreated-center conductor. (c) Untreated- right ground . (d) TS- left ground. (e) TS-center conductor. (t) TS- right ground. (g) VS- left ground. (h) VS----{;enter conductor . (i) VS-right ground. Note that the variation in thickness of the untreated CPW compared to the thickness of the smoothed CPWs.

loss increases as frequency increases. Therefore, smoothing processes may show even larger improvementfor electrical performance as frequency increases beyond 7 GHz. This could help enable customizable devices printed on-the-fly with selectable communication ability.

V. CONCLUSION

The inherent layer stacking and pointwise extrusion familiar to some **AM** processes render a component with much greater surface roughness than conventional manufactured components. This surface roughness reduces performance for many AM applications. Thermal and VS processes significantly decrease the undulating features of AM extruded surfaces. TS enhances the electrical performance for the CPWs studied here by decreasing insertion loss up to 40% at 7 GHz and achieving nearly isotropicperformance between perpendicular and parallel conductors printed on AM extruded substrates, which is favorable when designing printed electronics.VS also decreases insertion loss up to 24%, but still shows significant variation and unpredictability between conductor orientation. One would expect VS to outperform TS since the surface roughness is lower, but VS induces cracking of the conductive paste, which likely increases dissipative losses. Smoothing processes have the potential to open more widespread application space for customizable printed electronics devices.

R E FERENCES

[I] A. Bandyopadhyay, T. P. L. Gualtieri, and S. Bose, *Additive Manufacturing.* Boca Raton, FL, USA: CRC Press, 2016.

[2] E. Sachs, M. Cima, P. Williams, D. Brancazio, and J. Cornie, "Three dimensional printing: Rapid tooling and prototypes directly from a CAD model," *J. Eng. Ind.* , vol. 114, no. 4, pp. 481-488, Nov. 1992.

[3] A. Gebhardt, *Understanding Additive Manufacturing.* Munich, Germany: Carl Hanser Verlag, 2012.

[4] I. Gibson, D. W. Rosen, and B. Stucker, *Additive Ma1 1ufacturingTech - 11ologies: Rapid Prototyping to Direct Digital Manufacturing.* New York. NY, USA: Springer, 2010.

[5] N. Hopkinson, R. J. M. Hag,ue and P. M. Dickens, *Rapid Manufacturing: Ari Industrial Revolution for the Digital Age.* Hoboken, NJ, USA: Wiley, 2006.

[6] C. **M.** Neff, N. B. Crane, P. I. Deffenbaugh, J. L. Zunino, K. H. Church, and **M.** Newton, "Digital manufacturing and performance testing for military grade application specific electronic packaging (ASEP)," in *Proc.In!. Symp. Microelectron., Int. Microelectron. Assern. Packng. Soc.,* 2016, pp. 250-266.

[7] **K. H.** Church *et al.,* " Multimaterial and multilayer direct digital manufacturing of 3-D structural microwave electronics," *Proc. IEEE ,* vol. 105, no. 4, pp. 688--701, Apr. 2017.

[8] E. A. Rojas-Nastrucci *et al.,* "Characterization and modeling of k-band coplanar waveguides digitally manufactured using pulsed picosecond laser machining of thick-film conductive paste," *IEEE Trans. Mierow. Theory Techri.,* vol. 65, no. 9, pp. 3180-3187, Sep. 2017.

[9] D. Ahn, J.-H. Kweon, S. Kwon, J. Song, and S. Lee, "Representation of surface roughness in fused deposition modeling," *J. Mater. Process. Tech,wl.,* vol. 209, pp. 5593-5600, Aug. 2009.

[10] S.-H. Ahn, M. Montero, D. Odell, S. Roundy, and P. K. Wright, "Anisotropic material properties of fused deposition modeling ABS," *Rapid Prototyping J.,* vol. 8, no. 4, pp. 248--257, Oct 2002.

[11] K. M. Ashtankar, A. M. Kuthe, and B. S. Rathour, "Effect of build orientation on mechanical properties of rapid prototyping (fused deposition modelling) made acrylonitrile butad iene styrene (ABS) parts,"in *Proc. ASME ltll. Mech. Eng. Congr. Expo.,* San Diego, CA, USA, 2013, Art. no. VOi lT06A017.

[12] N. S. A. Bakar, M. R. Alkahari, and H. Boejang, "Analysis on fused deposition modelling performance," *J. Zhejiang Univ.-Sci. A,* vol. 11, no. 12, pp. 972- 977, 2010.

[13] A. Bellini and S. Gii(?lri, "Mechanical characterization of parts fabricated using fused deposition modeling," *Rapid Prototyping J.,* vol. 9, pp. 252- 264, 2003.
[14] P. M. Pandey, N. V. Reddy, and S. G. Dhande, "Virtual hybrid-FDM system to enhance surface finish," *Virtunl Phys. Prototyping,* vol. I, pp. 101- 116, Jun. 2006.
[15] S. Raul, V. S. Jatti, N. K. Khedkar, and T. P. Singh, "Investigation of the effect of built orientation on mechanical properties and total cost of FDM parts," *Procedia Mater.* Sci., vol. 6, pp. 1625-1630, 2014.
[16] B. Vasudevarao, D. P. Natarajan, M. Henderson, and A. Razdan, "Sensitivity of RP surface finish to process parameter variation," in *Proc. Solid Freeform Fabrication,* Austin, TX, USA, Aug. 2000, pp. 251- 258.
[17] Z. Cui, *Printed Electronics: Materials, Technologie,s & Applications.* Hoboken, **NJ,** USA: Wiley, 2016.
[18] D. P. Parekh, D. Cormier, and M. D. Dickey, *Additive Manufacturing.* Boca Raton, FL, USA: CRC Press, 2016.
[19] I. Nassar, H. Tsang, and T. Weller, "3D printed wideband harmonic transceiver for embedded passive wireless monitoring," *Electron. Letter,* vol. 50, no. 22, pp. 1609- 161I, 2014.
[20] J. M. O'Brien, J. E. Grandfield, G. Mumcu, and T. M. Weller, "Minia - turization of a spiral antenna using periodic Z-plane meandering," *IEEE Trans. Antennas Propag.,* vol. 63, no. 4, pp. 1843-1848, Apr. 2015.
[21] R. A. Ramirez, E. A. Rojas-Nastrucci, and T. M. Weller, "3D tag with improved read range for UHF rfid applications using additive manufacturing," in *Proc. IEEE 16th Annu. Wireless Mierow. Techrwl. Conf (WAMICON),* Apr. 2015, pp. 1-4.
[22] S. Kim, A. Shamim, A. Georgiadis, H. Auber,t and **M. M.** Tentzeris, "Fabrication of fully inkjet-printed vias and SIW structures on thick polymer substrates," *IEEE Trans. Compon., Packag,. Manuf Technol.,* vol. 6, no. 3, pp. 486-496, **Mar.** 20 I6 .
[23] S. Khan, N. Vahabisani, and **M .** Daneshmand, "A fully 3-D printed waveguide and its application as microfluidically controlled waveguide switch," *IEEE Trans. Compo,n. Packag,.Manuf Tec/mol.,* vol. 7, no. I, pp. 7 0.Jan. 2017.
[24] B. Zhang and **H.** Zirath, "Metallic 3-D printed rectangular waveguides for millimeter-wave applications," *IEEE Trans. Compon., Packag,. Manuf Tech,wl.,* vol. 6, no. 5, pp. 796-804, May 2016.
[25] G.-L. Huang, S.-G. Zhou, and T. Yuan, " Developmentof a wideband and high-efficiency waveguide-based compact antenna radiator with binder-jetting technique," *IEEE Trans. Compon., Packag., Mamif- Technol. ,* vol. 7, no. 2, pp. 254-260, Feb. 2017.
[26] **R. A.** Ramirez, E. A. Rojas-Nasrtucci, and T. M. Welle,r "UHF RFID tags for On-/Off-metal applications fabricated using additive manufacturing," *IEEE Antennas Wireless Propag. Lett.,* vol. 16, pp. 1635- 1638, 2017.
[27] E. A. Rojas-Nastrucci, J. T. Nussbaum, N. B. Crane, and T. M. Weller, "Ka-band characterization of binder jetting for 3-D printing of metallic rectangular waveguide circuits and antennas," *IEEE Trans. Mierow. Theory Tech11.,* vol. 65, no. 9, pp. 3099- 3108, Sep. 2017.
[28] D. Espalin, D. W. Muse, E. MacDonald, and R. B. Wicker, "3D Printing multifunctionality: Structures with electronics," *Int. J. Adv. Manuf Tec/mol.,* vol. 72, nos. 5- 8, pp. 963- 979, 2014.
[29] D. A. Roberson, R. B. Wicker, L. E. Murr, K. Church, and E. MacDonald, "Microstructural and process characterization of conductive traces printed from ag particulate inks," *Materials,* vol. 4, no. 6, pp. %3-979, 2011.
[30] T. P. Ketterl, "A 2.45 GHz phased array antenna unit cell fabricated using 3-D multi-layer direct digital manufacturing," *IEEE TrallS. Mierow. Theory Techt1.,* vol. 63, no. 12, pp. 4382-4394, Dec. 2015.
[31] S. P. Morgan, Jr, "Effect of surface roughness on eddy current losses at microwave frequencies," *J. Appl. Phys.,* vol. 20, no. 4, p. 352, 1949.
[32] T. C. Edwards and M. B. Steer, *Fowulatio11S for Microstrip Circuit Design,* 4th ed. Hoboken, **NJ,** USA: Wiley, 2016.
[33] A. Matsushima and **K.** Nakata, "Power loss and local surface impedance associated with conducting rough interfaces," *Electron. Conunun. Jpn. (Part II: Electron.,)* vol. 89, no. I, pp. 1- 10, 2006.
[34] A. Garg, A. Bhattacharya, and A. Batish, "On surface finish and dimensional accuracy of FDM parts after cold vapor treatment," *Mater. Manuf Processes,* vol. 31, no. 4, pp. 522- 529, 2015.
[35] C. Neff, M. Trapuzzano, and N. B. Crane, "Impact of vapor polishing on surface quality and mechanical properties of extruded ABS," *Rapid Prototyping J.,* vol. 12, no. 2, pp. 501- 508, 2017.
[36] D. F. Hawatrneh, S. LeBlanc, P. I. Deffenbaugh, and T. Weller, "Embedded 6-GHz 3-D printed half-wave dipole antenna," *IEEE Antennas Wireless Propag. Lett.,* vol. 16, pp. 145-148, 2017.
[37] J. W. Stratton, "A study of direct digital manufactured RF/microwave packaging," M.S. Thesis, Dept. Elect. Eng., Univ. South Florida, Tampa, FL, USA, 2015.
[38] D. Espalin, F. Medina, K Arcaute, B. Zinniel, T. Hoppe, and R. Wicke,r "Effects of vapor smoothing on ABS part dimensions," in *Proc. Rapid Conj. Expa,* Schaumburg 11., USA, May 2009, pp. 1- 17.
[39] R. Singh, S. Singh, and I. P. Singh, "Effect of hot vapor smoothing process on surface hardness of fused deposition modeling parts," *3D Printing Additive Manuf,* vol. 3, no. 2, pp. 128- 133, 2016.
[40] B. N. Turner and S. A. Gold, "A review of melt extrusion additive manufacturing processes: II. Materials, dimensional accuracy, and surface roughness," *Rapid Prototyping J.,* vol. 21, no. 3, pp. 250-261, 2015.
[41] D. M. Vincen,t"Vaporous solvent treatment of thermoplastic substrates," U.S. Patent 4529563 A, Jan. 5, 1985.
[42] J. Nussbaum and N. B. Cra,ne "Evaluation of processing variables in polymer projection sintering," *Rapid Prototyping J.,* vol. 24, no. 5, pp. 8 85, 2018.
[43] J. A. Jansen, "Environmental stress cracking the plastic killer," *Adv. Mater. Process.,* vol. 5, pp. 50-53, Feb. 2004.

Clayton Neff received the B.S., **M.S.,** and Ph.D. degrees in mechanical engineering from the University of South Florida, Tampa, FL, USA, in 2014, 2015, and 2018, respectively.

His graduate work concentrated on additive manufacturing of printed electronics with analysis on adhesion, electrical, thermal, and mechanical performance. In 2017 and 2018, he was an Air Force Research Laboratory Scholar with Eglin Air Force Base, Valparaiso, FL, USA, where he was involved in harsh environmental testing of printed electronics and development of adhesion test methods for printed electronic conductive inks. He currently holds a National Research Council post-<loctoral position with the Air Force Research Laboratory, Eglin Air Force Base, where he is involved in harsh environmental testing of embedded printed electronics.

Dr. Neff was a recipient of theOutstanding Graduate Scholar Award in 2018.

Eduardo A. Rojas-Nastrucci (S' 12- M'18) received the B.S. degree in electrical engineering from the Universidad de Carabobo, Valencia, Venezuel,a in 2009, and the M.S. and Ph.D. degrees in electrical engineering from the University of South Florida, Tampa, FL, USA, in 2014, and 2017, respectively.

In 2017, he joined the Embry-Riddle Aeronautical University (ERAU), Daytona Beach, FL, USA, where he is currently an Assistant Professor. He is currently the Director of ERAU's Wireless Devices and Electromagnetics Laboratory(WIDE Lab). He has authored or coauthored more than 28 peer-reviewed publications. He holds two U.S. patents and three active U.S. patent applications. His current research interests include microwave/mm-wave circuit and antenna applications of additive manufacturing and RFlD for wireless sensing.

Dr. Rojas-Nastrucci is a member of the IEEE MTT-S Technical Committee 24 and the RTCA SC-236 committee for Standards for Wireless Avionics Intra-Communication System (WAIC) within 4200-4400 MHz. He is a reviewer for the IEEE TRANSACTIONS ON MICROWAVE THEORY AND TECHNIQUES and the PROCEEDINGSOF THE IEEE.

Justin Nussbaum received the bachelor's, master's, and Ph.D. degrees in mechanical engineering from the University of South Florida, Tampa, FL, USA.

He became an expert in metal and polymer additive manufacturing with the University of South Florida. He developed an entirely new additive manufacturing technology out of industrial need. He is currently the Founder and CEO of Ascend Manufacturing, Knoxville, TN, USA, which designs and fabricates industrial additive manufacturing systems capable of the highest production speeds in the industry, unrivaled integrated QA/QC, and best-in-class material performance.

Darrell Griffin, photograph and biography not available at the time of publication.

T homas M. Weller (S'92- M'95-SM'98---F' 18) received the B.S., M.S., and Ph.D. degrees in electrical engineering from the University of Michigan, Ann Arbor, Ml, USA, in 1988, 1991, and 1995, respectively.

From 1988 to 1990, he was with Hughes Aircraft Company, El Segundo, CA, USA. From 1995 to 2018, he was a Faculty Member with the University of South Florida, Tampa, FL, USA. In 2018, he joined Oregon State University, Corvallis, OR, USA, where he is currently the Michael and Judith Gaulke Professor and the School Head of electrical engineering and computer science. He co-founded Modelithics, Inc., Tampa, in 2001. His current research interests include tunable and reconfigurable microwave circuits, microwave applications of additive manufacturing and 3-D printing, electromagnetic sensors, passive microwave circuit design, planar and 3-D electrically small antennas, and equivalent circuit modeling.

Nat han B. Crane received the B.S. and **M.S.** degrees in mechanical engineering from Brigham Young University, Provo, UT, USA, in 1998 and 1999, respectively, and the Ph.D. degree in mechanical engineering from the Massachusetts Institute of Technology, Cambridge, MA, USA, in 2005.

From 1999 to 2001, he was with Pratt & Whitney, Hartford, CT, USA. From 2005 to 2006, he was with the Sandia National Laboratories, Albuquerque, NM, USA. In 2006, he joined the University of South Florida, Tampa, FL, USA, as a faculty member. Since 2018, he has been with the Department of Mechanical Engineering, Brigham Young University, Provo, UT, USA, where he is currently a Professor. His current research interests include manufacturing process development based on surface tension phenomena and on additive manufacturing of metals and printed electronics.

Dr. Crane is a member of the American Society of Mechanical Engineers (ASME), where he has been a member of the MEMS Division Executive Committee since 2013. He was a recipient of the 2014 Fulbright Award, the 2015 USF Outstanding Faculty award, and the 2005 Solid Freeforrn Fabrication Symposium Outstanding Paper Award.